

Metallic evolution of small magnesium clusters

J. Akola^a, K. Rytönen, and M. Manninen

Department of Physics, University of Jyväskylä, P.O. Box 35, FIN-40351 Jyväskylä, Finland

Received 15 November 2000

Abstract. Structural and electronic properties of small magnesium clusters ($N \leq 13$) are studied using a first-principles simulation method in conjunction with the density functional theory and generalized gradient correction approximation for the exchange-correlation energy functional. It is observed that the onset of metallization of magnesium clusters is hard to assign since both the s - p hybridization and the energy gap between the valence and conduction bands do not evolve rapidly towards the known bulk properties. Instead these quantities show a slow and nonmonotonic evolution.

PACS. 36.40.Cg Electronic and magnetic properties of clusters – 36.40.Mr Spectroscopy and geometrical structure of clusters – 71.24.+q Electronic structure of clusters and nanoparticles

1 Introduction

The research of metal clusters has been highly motivated by the underlying jellium model (JM) which predicts a simple physical picture for the valence electrons [1]. The model has been most successful for the simple alkali metals (Na, K) but it has been applied also for other kinds of metals with a surprisingly good degree of agreement [2]. This suggests that the JM and especially its extension, deformed jellium model, is relatively inert to the perturbations (potential of ions, d -band etc.) caused by the actual metallic system.

Magnesium as a divalent metal is expected in some extent to differ from the JM predictions at small cluster sizes. At first the bonding between atoms is expected to be more van der Waals-like due to the filled electron subshell of Mg atom. An ideal example of this is the Mg₂ dimer which is very weakly bound and has a long bond length. The question now is where and how does the metallic character of Mg clusters arise? Studies concerning this issue were performed already a decade ago and the general conclusion was that the metallization of Mg clusters is a relatively slow process although also jellium-type magic clusters were observed [3–5].

In this article, we focus on the development of the metallic properties of small Mg clusters ($N \leq 13$) using a density functional theory based simulation method in conjunction with the recent PBE parametrization [9] of the gradient corrected exchange-correlation energy functional. Our aim here is to provide a complementary view of the metallization phenomena with respect to the previous studies [3–5] and gather information for future studies on larger Mg clusters. We see that theoretical studies in

this field are needed in conjunction with the experimental results which eventually are becoming available [6,7].

2 Method

The calculations are done using the BO–LSD–MD (Born-Oppenheimer local-spin-density molecular dynamics) method devised by Barnett and Landman, fully documented in Ref. [8]. In this method the ions move according to classical molecular dynamics in the force field calculated at each time step using the generalized gradient approximation (GGA) [9] for the exchange-correlation energy functional and pseudopotentials [10]. The electronic density as well as the auxiliary Kohn-Sham (KS) orbitals are augmented using a plane wave basis set (cutoff energy $E_{cut} = 15.4$ Ry) but we wish to stress that the method does not apply any of the standard supercell techniques in calculating the total energy of a finite system. Consequently, this allows us to study effectively also charged systems and systems possessing large multipole moments.

In practice, the problem of vast amount of different isomers is tackled by sampling the potential energy surface of neutral clusters by applying a so-called simulated annealing strategy where the system is simulated at high temperature and time-to-time cooled down. The corresponding structures are further optimized using a steepest-descent-like minimization procedure. Using neutral isomers as starting configurations also charged clusters (cations and anions) are optimized. During the simulations it became clear that the potential energy surfaces of Mg clusters are complicated due to the small energy differences between different isomers. This makes it a challenging task to find the ground state geometry especially at the larger cluster sizes ($N \geq 11$).

^a Present address: IFF, Forschungszentrum Jülich, D-52425 Jülich, Germany. e-mail: j.akola@fz-juelich.de

3 Results

The evolution of structural and electronic properties of small Mg clusters is illustrated in Fig. 1 and Table 1. The first implications of jellium-like behaviour are noticed as large binding energies (E_b) of Mg_4 and Mg_{10} clusters (8 and 20 valence electrons, respectively). Analyzation of the second derivative of the total energy ($-\Delta^2 E$) supports this conclusion and suggests a relative stability also for Mg_7 , Mg_9 and Mg_{11} clusters. Despite of the above jellium-type of indications, the general trend of the other properties in Fig. 1 (E_g , vIP, $\langle d \rangle$) does not imply an instantaneous or even rapid metallic evolution of Mg clusters. For instance, the vertical ionization potential (vIP) of Mg_4 shows an anomalous dip although it should be a local maximum according to the JM. This can be understood by considering that a single Mg atom possesses a high IP value (experimental value 7.64 eV [11]) due to its closed subshell. This should be reflected also in the small cluster regime whenever the charge localization picture is valid. According to the average nearest-neighbour distances ($\langle d \rangle$) Mg_4 is more tightly packed than its neighbours which implies a stronger charge delocalization and consequently a lower vIP value. The $\langle d \rangle$ value of Mg_{10} indicates a similar kind of phenomenon although in this case the vIP value is not smaller than that of the neighbouring cluster sizes.

It is evident from the Fig. 1 that the metallic evolution of Mg clusters is neither rapid nor a monotonic process. Despite Mg_4 and Mg_{10} , the clusters do not generally fit to the simple jellium description but show electronic properties pertaining to a more localized electron density (*e.g.* long bond lengths and high vIP values). This is valid even for the largest clusters ($N \geq 11$) where the bond distances are only 2% shorter than for the Mg bulk (see Table 1) and the HOMO-LUMO gaps (especially for Mg_{11}) are still considerably large.

In order to gain a more profound insight to the metallic evolution of Mg clusters we have studied the $s-p$ hybridization of occupied KS orbitals by expanding them onto a basis set consisting of spherical harmonics. This analysis is performed with respect to all the atoms in the cluster (by repeating the procedure in a finite sphere for every atom, respectively, and calculating the weighted average of the particular KS orbital over atoms). The resulting s - and p -components are shown in Table 1. When inspecting these numbers one should remember that in the case of Mg the hybridization of s - and p - bands occurs first near the Fermi energy. Therefore, the lowest s -component values (seen as the lower-boundary) usually correspond to the HOMO orbital. From Tab. 1 it is obvious that the $s-p$ hybridization gradually increases throughout the whole set of data and that no drastic onset for hybridization can be observed. However, visible increases of p -component are noticed for Mg_4 and Mg_{10} clusters supporting our observations of the unique nature of these clusters. Furthermore, we remark that the rapid increase of the upper-bound of p -component after Mg_8 correlates with the change in the structural motifs (see the discussion below).

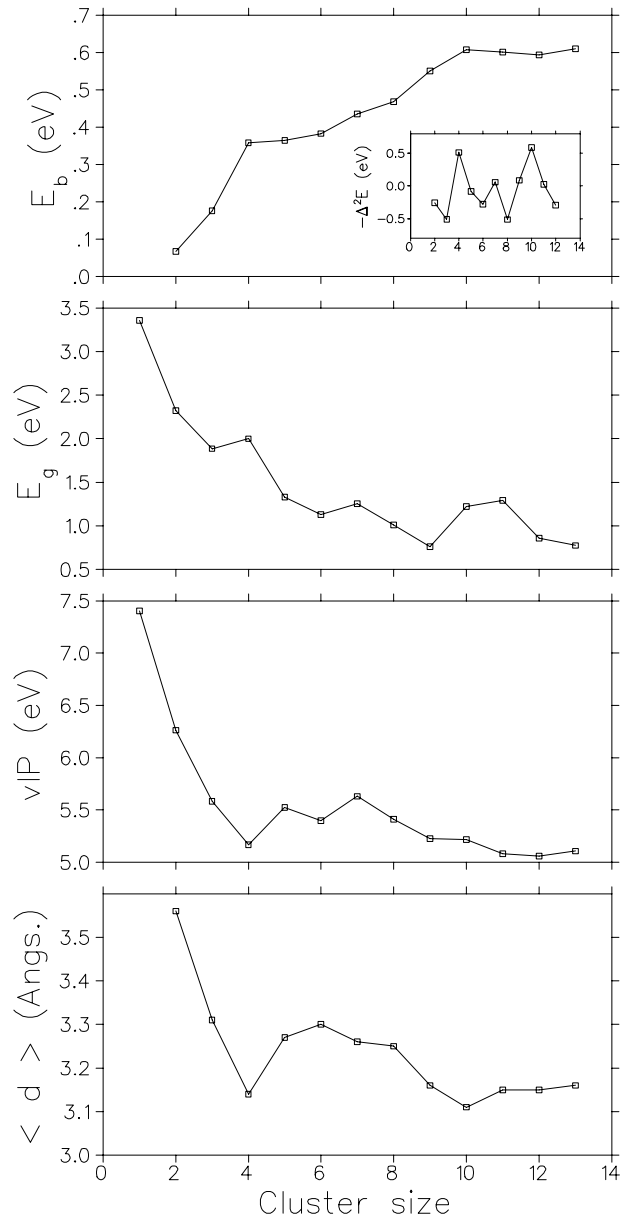


Fig. 1. Properties of small Mg clusters. From top to bottom: Binding energies (E_b), second derivatives of total energies ($-\Delta^2 E$), HOMO-LUMO gaps (E_g), vertical ionization potentials (vIP) and average nearest neighbour distances ($\langle d \rangle$).

The first structural trend of Mg clusters starts from Mg_4 (tetrahedron) and continues up to Mg_8 . The cluster geometries in this domain consist of fused tetrahedrons which *e.g.* in the case of Mg_7 lead to the relatively stable decahedron confinement (see binding energies in Fig. 1). After Mg_8 another competing motif based on the six atom trigonal prism core dominates the cluster growth up to Mg_{13} (see Fig. 2) which was the largest cluster size studied extensively in this work. We remark that concerning cluster geometries our results corroborate the earlier findings [3–5] although for Mg_{12} and Mg_{13} we obtain slightly different lowest energy minima. We also notice that the overall geometries of magic Mg_4 and Mg_{10} clusters are

Table 1. Properties of magnesium clusters. In addition to Fig. 1 also adiabatic ionization potential (aIP), vertical detachment energy (vDE), and *s*- and *p*-components of occupied KS orbitals are shown. Bulk values are obtained from Ref. [11] (E_b), Ref. [12] (vIP, $\langle d \rangle$) and Ref. [13] (*s*- and *p*-components of DOS at Fermi energy).

Cluster size	E_b (eV)	$-\Delta^2 E$ (eV)	E_g (eV)	vIP (eV)	aIP (eV)	vDE (eV)	$\langle d \rangle$ (Å)	<i>s</i> -component	<i>p</i> -component
1			3.36	7.40				1.00	0.00
2	0.07	-0.26	2.32	6.26	6.13		3.56	0.96	0.04
3	0.18	-0.51	1.89	5.59	5.44		3.31	0.89 - 0.90	0.09 - 0.10
4	0.36	+0.51	2.00	5.17	4.99		3.14	0.80 - 0.83	0.15 - 0.18
5	0.36	-0.08	1.33	5.53	5.30		3.27	0.76 - 0.90	0.08 - 0.22
6	0.38	-0.28	1.13	5.40	5.24		3.30	0.76 - 0.89	0.08 - 0.22
7	0.44	+0.06	1.26	5.63	5.26		3.26	0.72 - 0.83	0.16 - 0.25
8	0.47	-0.51	1.01	5.41	5.16	1.69	3.25	0.70 - 0.84	0.15 - 0.26
9	0.55	+0.09	0.76	5.23	5.09	1.96	3.16	0.60 - 0.84	0.15 - 0.36
10	0.61	+0.59	1.22	5.22	5.09	1.68	3.11	0.47 - 0.85	0.15 - 0.46
11	0.60	+0.02	1.29	5.08	4.75	1.88	3.15	0.48 - 0.85	0.13 - 0.46
12	0.59	-0.29	0.86	5.06	4.80	1.82	3.15	0.53 - 0.86	0.14 - 0.42
13	0.61		0.78	5.11	4.99	1.84	3.16	0.48 - 0.86	0.14 - 0.48
Bulk	1.51			3.64		3.64	3.21	0.34	0.50

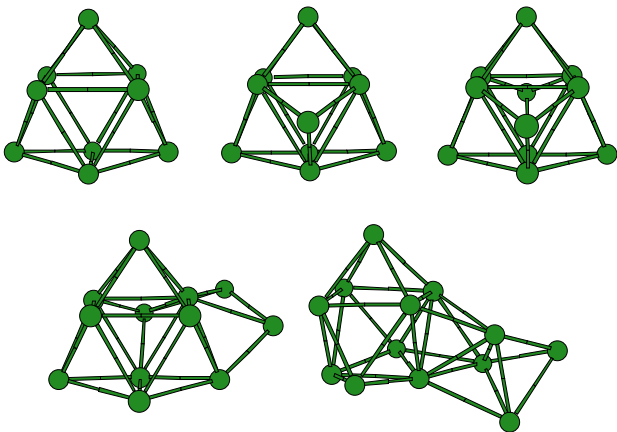


Fig. 2. The lowest energy structures of Mg_9 - Mg_{13} clusters. Note the presence of the trigonal prism unit in all the clusters.

tetrahedral, *i.e.* they are octupole deformed with respect to the spherical shape. According to the deformed JM this kind of confinement has the same magic numbers 8, 20 and 40 for the valence electrons as the spherical JM [14, 15]. Indeed, this finding supports the conclusion made by Reimann *et al.* [14] of the tetrahedral shapes of magic Mg clusters, although the geometry of Mg_{10} is not an exact tetrahedron. We have also studied the tetrahedral deformation of Mg_{20} . In our calculations the nearly spherical lowest-energy geometry of Mg_{20} found by Delaly *et al.* [4] experiences an octupole deformation in agreement with the discussion above. However, the resulting total energy is significantly better than that for the perfect Mg_{20} tetrahedron.

In addition to neutral Mg clusters, we have also studied cations ($N = 1 - 13$) and anions ($N = 8 - 13$) and the resulting electron ionization/detachment energies with re-

spect to the neutral clusters (see Table 1). During this work it became evident that the PBE parametrization (as well as all the other LDA/GGA based parametrizations) of the exchange-correlation functional results positive HOMO eigenenergies for the smallest cluster anions and therefore we report our results only for the larger Mg anions ($N \geq 8$) where this deficiency is not present. We perceive that the overall geometries of charged clusters differ from the corresponding neutral ones in many cases. For example, the cations prefer linear geometries up to Mg_4^+ and the lowest-energy geometry of Mg_9^+ is still tetrahedrally packed (bicapped decahedron). For the largest sizes ($N = 11 - 13$) the potential energy surface is complex due to the very small energy differences between different isomers, and therefore it is not surprising to observe differences between neutral and charged lowest-energy geometries. Nevertheless, we observe that the lowest-energy structures of Mg_{12}^- , Mg_{13}^+ and Mg_{13}^- are based on the corresponding neutral lowest-energy geometry.

In Figure 3, we present the density of occupied KS states (DOS) of the lowest-energy Mg_9^- - Mg_{13}^- isomers. Based on our earlier experience with small Al clusters [16,17], we presume that a relatively good approximation for the experimental low-temperature photoelectron spectrum (PES) is obtained by shifting the KS energies (peaks) by the asymptotic exchange-correlation potential v_{xc}^∞ which consists mainly of the self-interaction correction of the specific KS-orbital. Since v_{xc}^∞ of simple metals [17] depends only slightly on the KS orbital in question, we suggest that a simple first prediction for the experimental PES of Mg clusters is obtained by shifting the whole DOS by the v_{xc}^∞ value of the HOMO orbital (calculated values for the shift are given in the caption of Fig. 3). We wish to point out here that the DOS is very sensitive to the detailed ionic structure of the cluster, and therefore experimental PES can be used for structure determination.

It is observed from Fig. 3 that the DOS of Mg_9^- and Mg_{10}^- are relatively simple due to the symmetric cluster

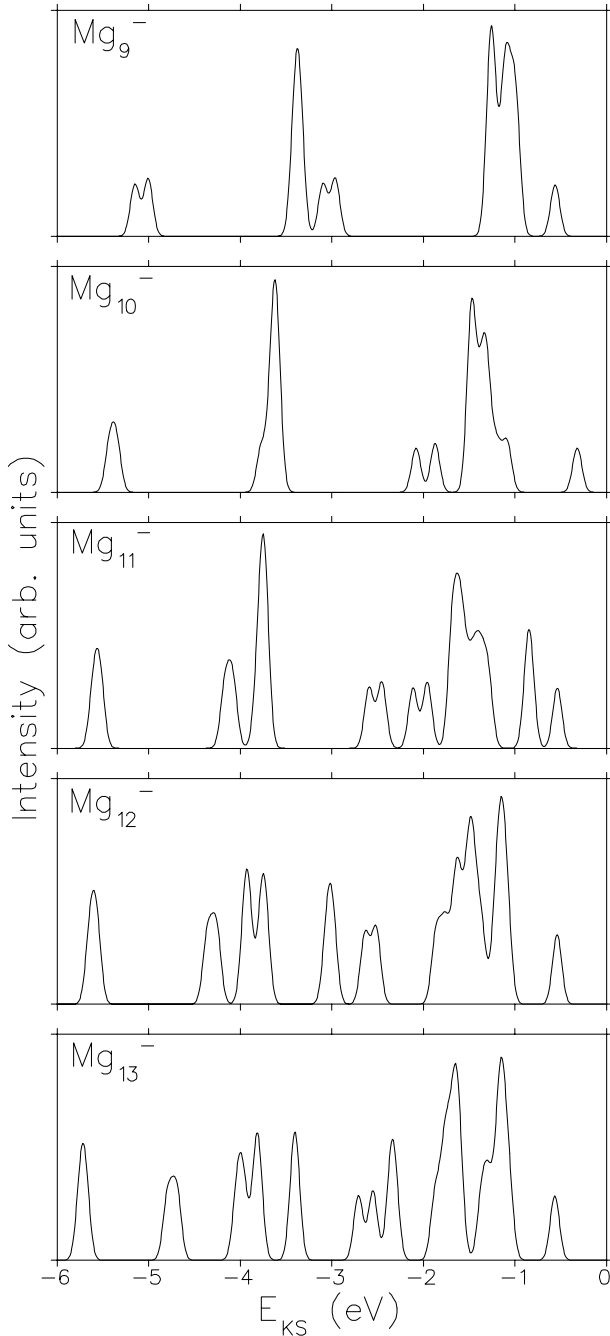


Fig. 3. Density of KS states of $\text{Mg}_9\text{-Mg}_{13}$ clusters. Note that a simple theoretical estimate for the experimental PES can be obtained by shifting the distributions by -1.40 , -1.36 , -1.34 , -1.28 , and -1.27 eV, respectively. Note also that the geometry of Mg_{11}^- corresponds to a different isomer than that presented in Fig. 1.

geometries and due to the shell closure at 20 valence electrons. For the larger sizes the symmetry is lower and the DOS shows correspondingly a more complex structure. We also remark that the energy gap between the HOMO (conduction band) and the underlying orbitals (valence band) is largest for Mg_{10}^- in agreement with the JM, but is considerable also for the other anions.

4 Conclusion

In this article, we have reported our findings on the metallization of small Mg cluster. It is observed that according to the $s-p$ hybridization and the band gap between valence and conduction bands the metallic character of Mg cluster evolves slowly and nonmonotonically, and that this process is not completed even for Mg_{13} . The incomplete metallization is also reflected by the interesting lowest-energy geometries of $\text{Mg}_{11}\text{-Mg}_{13}$, which are based on capping the magic Mg_{10} cluster. The remaining questions are now: How do the metallic properties of Mg clusters develop after Mg_{13} and what are the structural trends? It would be interesting to study these questions by applying new indicators for the metallization (*e.g.* charge localization) and to expand the range of cluster sizes presented in this article. Also the new experimental results [6, 7] confirm that more theoretical work is needed on Mg clusters.

We wish to thank U. Landman for suggesting us to study Mg clusters and H. Häkkinen for several valuable discussions. J.A. gratefully acknowledges a grant from the Väisälä foundation. This work has been supported by the Academy of Finland under the Finnish Centre of Excellence Programme 2000-2005 (Project No. 44875, Nuclear and Condensed Matter Programme at JYFL).

References

1. M. Brack, *Rev. Mod. Phys.* **65**, 676 (1993).
2. W.A. de Heer, *Rev. Mod. Phys.* **65**, 611 (1993).
3. F. Reuse *et al.*, *Phys. Rev. B* **41**, 11743 (1990).
4. P. Delaly *et al.*, *Phys. Rev. B* **45**, 3838 (1992).
5. V. Kumar, R. Car, *Phys. Rev. B* **44**, 8243 (1991).
6. K. Bowen, contribution to ISSPIC10.
7. T. Diederich *et al.*, *Phys. Rev. Lett.* **86**, 4807 (2001).
8. R.N. Barnett, U. Landman, *Phys. Rev. B* **48**, 2081 (1993).
9. J.P. Perdew *et al.*, *Phys. Rev. Lett.* **77**, 3865 (1996); *ibid.*, **78**, 1396(E) (1997).
10. N. Troullier, J.L. Martins, *Phys. Rev. B* **43**, 1993 (1991). For the magnesium $3s^2$ valence electrons, we use s -nonlocal and p -local components with cut-off radii of 2.5 and $2.75a_0$, respectively.
11. C. Kittel, *Introduction to Solid State Physics*, 7th edn. (John Wiley & Sons, New York, 1996).
12. N.W. Ashcroft, N.D. Mermin, *Solid State Physics* (International Edition, Saunders College Publishing, New York, 1976).
13. R.P. Gupta, A.J. Freeman, *Phys. Rev. Lett.* **36**, 1194 (1976).
14. S.M. Reimann *et al.*, *Phys. Rev. B* **56**, 12147 (1997).
15. The spherical harmonics analysis of Mg_4 and Mg_{10} clusters with respect to the center of mass of the cluster shows only minor deviations in the KS orbital characters with respect to the spherical JM picture.
16. J. Akola *et al.*, *Phys. Rev. B* **60**, 11297 (1999).
17. J. Akola *et al.*, *Phys. Rev. B* **62**, 13216 (2000).